Fukuyama-type congenital muscular dystrophy (FCMD; MIM 253800) is an autosomal recessive disorder and the second most common muscular dystrophy, following DMD, in Japan [1]. Clinical manifestations of FCMD include severe muscle wasting from early infancy with malformation of the brain and eyes. We previously isolated the responsible gene for FCMD, termed *fukutin* [2,3]. Fukutin presumably modulates the glycosylation of α-dystroglycan (α-DG), one of the major components of the dystrophin–glycoprotein complex, since α-dystroglycan is hypoglycosylated in FCMD muscle [4,5]. Fukutin-mediated glycosylation is crucial for binding of α-DG to ECM proteins such as laminin, agrin, and perlecan, which are important for maintaining muscle cell integrity [5]. Hypoglycosylation of α-DG is likely to attenuate the stable connection between skeletal muscle sarcoplasmic membrane and the basement membrane. This architectural and functional instability of muscle fibers is presumed to induce severe muscular dystrophy in FCMD [4,6].

Accumulating evidence indicates that hypoglycosylation of α-DG underlies a number of muscular dystrophies. Hypoglycosylated α-DG provokes the post-translational disruption of dystroglycan-ligand interactions in skeletal muscle, leading to the severe phenotypes of congenital muscular dystrophies [7]. Mutations in glycosyltransferases have been linked to several muscular dystrophies, including POMGnT1 (protein *O*-mannose β-1, 2-*N*-acetylglucosaminyltransferase 1) with muscle–eye–brain disease; POMT1/2 (protein *O*-mannosyltransferase 1/2) with Walker–Warburg syndrome; FKRP (fukutin-related protein) with congenital muscular dystrophy type 1C (MDC1C). In addition, mutations in the putative glycosyltransferase LARGE correlate with myodystrophy in mice and human congenital muscular dystrophy 1D (MDC1D) [8–13].

Another congenital muscular dystrophy, laminin-α2 deficient congenital muscular dystrophy (MDC1A), is one of the most common childhood congenital muscular dystrophies in the European population [14]. MDC1A is an autosomal recessive disorder that is caused by mutation of the *LAMA2* gene [15]. Clinical muscular features of MDC1A are grossly identical to the FCMD phenotype and characterized as severe neonatal hypotonia. Laminin-α2 is the main component of the basement membrane and plays an essential role in its formation, serving as a signaling molecule to interact with other ECM or sarcoplasmic membrane components [16]. α-DG is a primary receptor for laminin-α2 on the sarcoplasmic membrane [17,18]. Thus, attenuated connections between laminin and α-DG might account for muscular dystrophy in MDC1A.

Although DMD and these CMDs are categorized into the same clinical entity, 'muscular dystrophies,' manifestations of CMDs are known to differ from those of DMD in several ways. First, patients with CMDs show congenital anomalies in muscle pathology, implying developmental defects in CMD muscle [19]. Second, these CMDs show severe pathological changes in the early infantile period with almost fixed characteristics thereafter, unlike the later onset and progressive features of DMD [1]. Finally, the pathophysiology of CMD muscle is characterized by few active dystrophic and regenerating fibers, correlating with moderate increases in serum CK levels [1]. In contrast, muscle specimens from DMD patients show severe necrotic changes and active regeneration, both of which are evidenced by extremely high serum CK levels.

Dystrophic features in CMD have been defined by the observation of 'opaque fibers' in biopsied specimens, which are suggested to indicate pre-necrotic fibers like those often seen in DMD muscle. Opaque fibers in CMD biopsied muscle specimens are unexpectedly prominent, considering the moderate serum CK levels. However, we suspect that the opaque fibers are artificially generated by the biopsy itself, due to the technical tension placed on fragile CMD muscle membranes (unpublished data). Therefore, the pathological characteristics of these CMDs are not likely the same as those of late-stage DMD. The pathophysiological and molecular mechanisms of these CMDs deserve further investigation.

Although gene expression profiling of DMD skeletal muscle has been described previously [20–22], neither FCMD nor MDC1A has been characterized. To investigate the molecular mechanisms of CMDs relative to DMD, we profiled gene expression in FCMD and MDC1A muscle using a custom cDNA microarray. Profiles were analyzed by a multi-dimensional statistical analysis, the Distillation, to extract determinant genes, revealing a more detailed molecular mechanism for these CMDs.

Materials and methods

Patient materials. All clinical materials were collected for diagnostic purposes. Four muscle specimens (biceps branchii) from FCMD patients (F1–F4) and one from MDC1A (M1) were used in the analysis (Fig. 1). Genetic screening identified a homozygous retrotransposal insertion into the 3′ untranslated region of *fukutin* in all patients [3]. For MDC1A, the patient showed a typical disease onset, and the specimen was negative for anti-laminin-α2 staining. We used pooled muscle RNA (Origene Technologies) as an internal standard for microarray experiments. For age-matched non-dystrophic controls, muscle RNA from two children was used (C1 and C2, 1 year old, and 7 years old, respectively). These two samples were selected based on normal laboratory findings, normal plasma CK levels, and no histological findings of muscular dystrophy.

Histological analysis. Serial sections from the biopsied cryospecimen used for microarray experiments were stained with hematoxylin and eosin by standard methods. Scion Image Beta 3b (Scion) was used for the two-dimensional morphometric analysis of muscle specimen. For each cryospecimen, ten pictures were taken randomly. We measured the area of muscle tissue, adipose tissue, and the remaining interstitial tissues, and then measured the average cross-sectioned muscle fiber diameters. Statistical analysis was performed using Student's t test ($p < 0.005$).

RNA isolation and expression profiling. Generation of cDNA microarrays of skeletal muscle transcripts has been reported previously [22]. Using a similar method, we constructed a cDNA chip containing 5600 genes expressed in skeletal muscle. RNA isolation, hybridization, and detection methods also have been previously reported. Microarray experiments were carried out using a competitive hybridization method with two labeled targets: one for muscle RNAs from FCMD, MDC1A or normal controls, and another for pooled muscle RNA (Origene), which

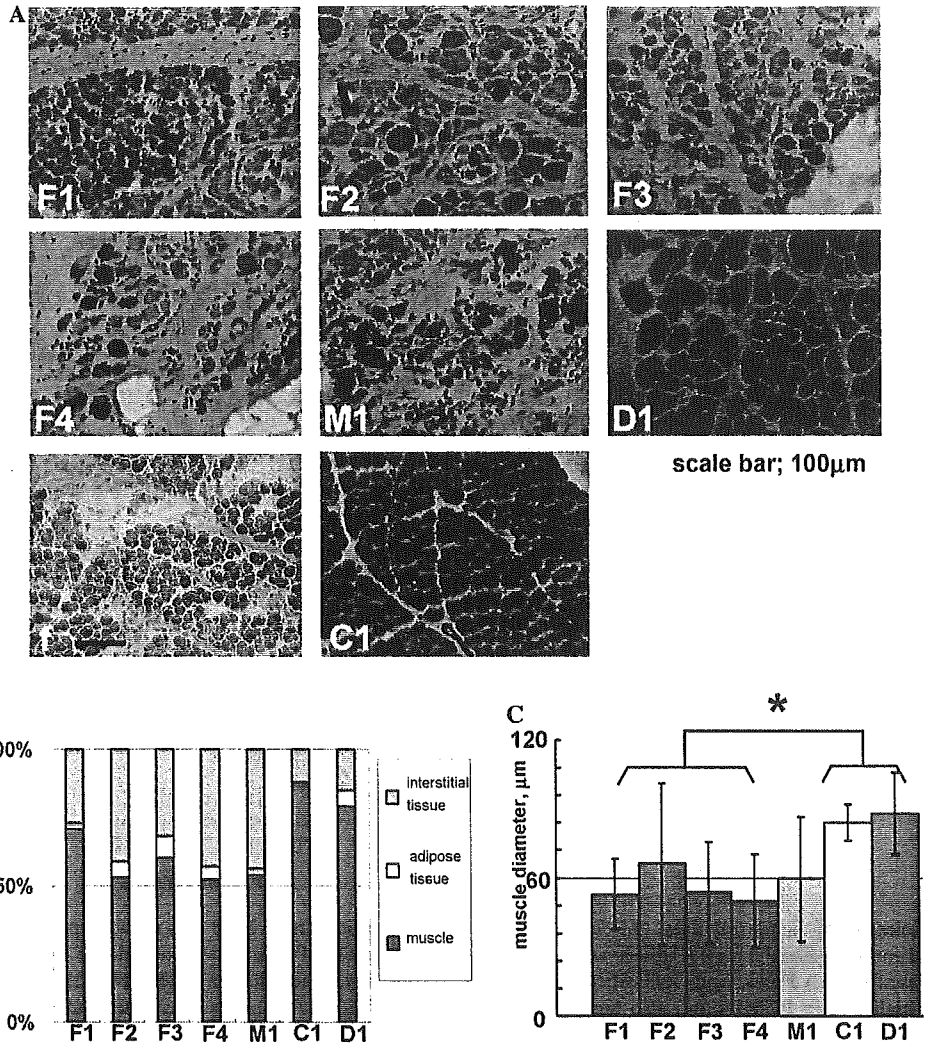

Fig. 1. Morphometric analysis of FCMD and MDC1A skeletal muscle. (A) HE stain of biopsied skeletal muscle used for further analysis (F1–F4 and M1). For comparison, DMD muscle and skeletal muscle from normal fetus (f, 21 weeks) are shown. Note that fetal tissue is quite similar to F1–F4. Fibrosis exists in F1 patient, though necrotic lesions are not prominent in F2–F4 and in M1. Extremely thin muscle fibers with high nuclear to cytoplasmic contents are seen. FCMD-1 (F1, 20 days), FCMD-2 (F2, 7 months), FCMD-3 (F3, 1 year 4 months), FCMD-4 (F4, 1 year 6 months), MDC1A-1 (M1, 1 year 8 months), DMD (D1, 1 year), and normal control (C1, 1 year). Scale bar = 100μm. (B) Components of each skeletal muscle (muscle components, interstitial tissue, and adipose tissue) were calculated for FCMD-1, FCMD-2, FCMD-3, FCMD-4, MDC1A-1, normal control, and DMD-1. Note that interstitial components are prominent in F1–F4 and M1. (C) Diameter of skeletal muscle fiber. The mean diameters of F1–F4 and M1 are significantly smaller than those of the age-matched control (C1) and DMD muscle (D1) (*$p < 0.005$). The variance of the diameter also is high in FCMD and MD muscle fibers.

served as an internal control for per-chip normalization. Hybridization was conducted at least twice. Hybridization intensities of each spot and background intensities were calculated and normalized using ScanArray 5000 with Quant Array software (Perkin-Elmer Life Science).

Statistical analysis. Analysis of microarray data was performed using Microsoft Excel (Microsoft) and Genespring software version 6.2 (Silicon Genetics). Data used for further analysis were calculated using a previously reported method [22]. To avoid 'false positive' signals, we excluded genes from the analysis for which average normal expression level constraints are under 500. Next, per spot and per chip, intensity dependent (Lowess) normalization was performed to minimize the variation in each microarray experiment. The average expression signal compared to pooled muscle RNA of each gene signal was estimated as the fold ratio. Two thousand three hundred and forty-five genes were selected for further analysis. The correlation coefficient for each signal between FCMD, MDC1A, and normal controls was calculated using Microsoft Excel for 688 genes whose expression level is reproducible (p-value $t < 0.05$).

To extract genes that characterize the expression profile of FCMD and MDC1A skeletal muscle compared to normal muscle, we adopted an original statistical analysis method, the Distillation [23]. Using this analysis, we could find genes whose expression pattern significantly distinguishes a certain disease from others. This analysis also sorts paired genes whose mutual expression patterns can discern one disease or normal control from another.

Quantitative real-time PCR. To confirm the microarray data, we performed real-time quantitative PCR. We produced single-strand cDNA with random primers, and quantitative real-time RT-PCR using SYBR-green was performed using the ABI Prism 7900 sequence detection system (Applied Biosynthesis). Primer sequences were as follows.

Gapdh: forward 5′-CATCTTCCAGGAGCGAGATC, reverse 5′-TGCAAATGAGCCCCAGCCTT; *TNNT2:* forward 5′-ATCAATGTTCTCCGAAACAGGATCAA, reverse 5′-GAGGAGCAGATCTTTGGTGAAGGA; *CGI-38*: forward 5′-CTCGGGTCATCAACTATGAGGAGTTCAA, reverse 5′-CTACAGCACCCCCTGTTTTTGCTTTAGT; *sarcoglycan* β forward 5′-AGCCTATTGTTTTTCAGCAAGGGACAAC, reverse

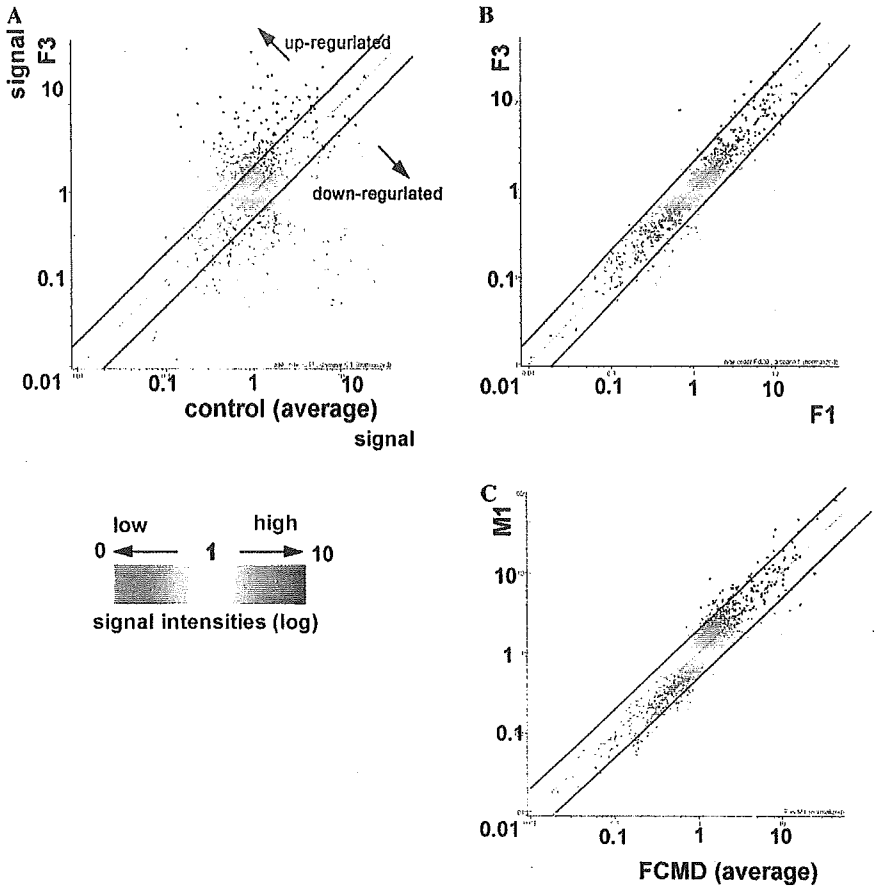

Fig. 2. Correlation co-efficiencies of microarray data. (A) Scatter graph of a cDNA microarray. Each axis shows expression signal intensities. *X* Axis, signal intensities of normal control skeletal muscle (C, the average signal of normal controls); *Y* axis, signal intensities of F3. (B) *X* axis, signal intensities of F1; *Y* axis, signal intensities of F3. (C) *Y* axis, signal intensities of M1; *X* axis, average signal intensities of F1–F4. Note that the correlation co-efficiency of microarray data is quite high among FCMDs and also high between FCMD and MDC1A samples. Blue lines show 2-, 1-, and 0.5-fold increases, respectively.

Table 1
Correlation coefficient of data from each microarray experiment

Sample No.	Age	C1 1y	C2 7y	F1 20d	F2 7m	F3 1y4m	F4 1y6m	M1 8m
C1	1y	1	0.97	0.6	0.42	0.53	0.32	0.42
C2	7y	0.95	1	0.6	0.44	0.55	0.33	0.45
F1	20d	0.65	0.67	1	0.84	0.87	0.77	0.82
F2	7m	0.47	0.53	0.9	1	0.88	0.85	0.83
F3	1y4m	0.57	0.64	0.93	0.93	1	0.78	0.86
F4	1y6m	0.38	0.45	0.84	0.91	0.9	1	0.76
M1	8m	0.49	0.56	0.89	0.9	0.92	0.87	1

5′-TTTTCACTCCACTTGGCAAATGAAACTC; *MYH2:* forward 5′-AGTTCCGCAAGGTGCAGCACGAGCT, reverse 5′-CCACCTAAAGGGCTGTTGCAAAGGC.

Statistical analysis was performed with Student's *t* test, using duplicate experiments of two patients for each disease and normal control.

In situ hybridization. In situ hybridization was performed according to standard methods. Sense and anti-sense sequence templates (*collagen3a*, *collagen15a1*, *Thrombospondin-4*, and *osteoblast-specific factor-2*) containing T7 or SP6 promoters were produced through PCR, and digoxigenin-labeled RNA probes were generated by transcribing with T7 or SP6 RNA polymerase. Sliced cryosections (8 μm) of skeletal muscle from FCMD (1 year of age) and a normal control (1 year of age) were fixed with 4% paraformaldehyde for 30 min. After treatment with proteinase K (0.5 μg/mg) for 5 min, samples were overlaid with hybridization solution containing digoxigenin-labeled probe. Hybridization signals were detected according to manufacturer's instructions.

Results

FCMD and MDC1A skeletal muscle are histologically distinct from DMD

We performed histological examination to document the characteristics of skeletal muscle samples used for

microarray expression analysis. Skeletal muscle samples from four FCMD patients and one MDC1A patient were obtained via biopsy at various ages during childhood (Fig. 1). In all CMD samples, histological examination revealed dystrophic features and marked variations in fiber size with less evidence of severe necrotic and regenerating fibers, prominent interstitial tissues, and adipose tissue proliferation (Fig. 1A, F1–F4, M1).

Abundant interstitial tissue was the most characteristic feature in all samples, appearing as early as 20 days of age (Fig. 1A, F1). To quantify the extent of interstitial tissue, we measured the areas of muscle, lipid, and

Table 2a
Genes up-regulated in both FCMD and MDC1A skeletal muscle

Genbank Nos.	Product	Common name	Fold change	
			FCMD	MDC1A
Muscle components				
NM_005159	Actin, α, cardiac muscle precursor	*ACTA*	5.1	8.3
NM_004997	Myosin-binding protein H	*MYBPH*	9.4	6.7
NM_003063	Sarcolipin	*SLN*	9.1	9.6
NM_005022	Profilin 1	*PFN1*	6.6	4.5
XM_010544	*N*-Acetylgalactosaminyltransferase 7	*GALNT7*	6.5	9.5
NM_003186	Transgelin	*TAGLN*	4.2	8.7
NM_001614	Actin, γ1 propeptide	*ACTG*	5.8	8.6
NM_004393	Dystroglycan 1 precursor	*DAG1*	1.5	1.6
ECM components				
NM_000090	α1 type III collagen preproprotein	*COL3A1*	50.1	54.6
NM_003248	Thrombospondin 4	*THBS4*	50	154.6
NM_006475	Osteoblast-specific factor 2	*OSF-2*	20.3	28.1
NM_003380	Vimentin	*VIM*	13.5	18.2
NM_002295	Laminin receptor-1 (67kD)	*LAMR1*	12.3	5.4
NM_003118	Osteonectin	*SPARC*	11.9	26.5
M55270	Matrix Glia protein	*MGP*	11.4	7.3
XM_045926	Lumican	*LUM*	11.2	31.9
NM_002727	Proteoglycan 1, secretory granule	*PRG1*	5.2	4.0
NM_005507	Cofilin 1 (non-muscle)	*CFL1*	4.6	5.7
NM_005410	Selenoprotein P precursor	*SEPP1*	4.5	4.6
NM_002292	Laminin, β 2 precursor	*LAMB2*	3.3	2.2
NM_000426	Laminin, α-2 (merosin)	*LAMA2*	2.9	0.8
NM_000419	Integrin β 1 (fibronectin receptor)	*ITGB1*	2.9	4.2
NM_032470	Tenascin XB, isoform 2	*TNXB*	2.7	6.5
Cell differentiation and adhesion				
X02508	Acetylcholine receptor (AChR) α subunit	*ACHR*	25.9	20.2
NM_000041	Apolipoprotein E	*APOE*	14.8	8
NM_000079	Cholinergic receptor, nicotinic, α precursor	*CHRNA1*	11.3	7.3
NM_002970	Spermidine/spermine N1-acetyltransferase	*SAT*	8.9	11.6
NM_001553	Insulin-like growth factor binding protein 7	*IGFBP7*	7.4	6.8
AF144103	NJAC protein	*NJAC*	2.8	4.3
NM_002402	Mesoderm-specific transcript (mouse) homolog	*MEST*	5.6	6.1
NM_000919	Peptidylglycine α-amidating monooxygenase	*PAM*	5.5	10.8
NM_000700	Annexin I	*ANXA1*	5.1	11.6
NM_001129	Adipocyte enhancer binding protein 1	*AEBP1*	3.8	21.3
Immune related				
M27635	Lymphocyte antigen	*HLA-DRw12*	10.2	3.6
NM_022555	Major histocompatibility complex	*HLA-DRB3*	10.1	3.9
Others, EST				
L01124	Ribosomal protein S13	*RPS13*	6.5	8.1
BC005863	Ribosomal protein, large, P0	*RPP0*	6.3	4.6
NM_00597	Calcium-binding protein A13	*S100A13*	5.2	6.2
NM_006000	Tubulin, α1	*Tuba1*	5	6.1
EST				
AL049455	Unknown	*dkfzp586d2322*	4.4	17.2
AL038078	Unknown	*dkfzp566k121*	7.2	9.8
Glycosyltransferase				
NM_018446	Glycosyltransferase AD-017	*AD-017*	1.5	2.8
XM_003527	*N*-Acetylgalactosaminyltransferase 7	*GalNac*	1.9	2.3
NM_005827	UDP-galactose transporter related	*UGTREL1*	1.3	1.3

connective tissue in each sample specimen using Scion Image (Fig. 1B). The relative area of interstitial tissues varied but did not correlate with patient age. Inflammation and regeneration were less apparent. In all samples examined, necrotic fibers were rare compared with DMD (Fig. 1A, D1). It is noteworthy that necrotic lesions are the least severe in F1 despite the abundance of interstitial tissue.

Next, we measured the cross-sectioned diameter of each muscle fiber. Diameters of FCMD and MDC1A muscle fibers are significantly smaller than those of normal sample fibers at 7 months of age (Fig. 1A, C1, and C; Student's t test, $p < 0.005$). Size variability among muscle fibers was remarkable in the CMDs (Fig. 1C). Some fibers were too thin to analyze, indicating immature, poor muscle components. In contrast, DMD muscle fibers exhibited degeneration and necrosis of muscle fibers accompanied by active regeneration (Fig. 1A, D1). These observations suggest that active regeneration and degeneration, which are characteristic of classical muscular dystrophies, might not be a primary feature of FCMD and MDC1A.

Overall gene expression profiles are highly similar among CMDs, regardless of pathological changes

We analyzed gene expression profiles of CMD skeletal muscle and normal controls to assess the correlation of histological features with gene expression. Scatter graphs of expression data were created for general comparison of expression profiles. The lack of concordance between FCMD and control data indicates the altered expression of numerous genes in disease muscle (Fig. 2A). In contrast, comparison of any two FCMD samples showed good concordance (Fig. 2B), and we observed high correlation among all FCMD cases regardless of pathological differences. We then calculated the correlation co-efficiency of microarray data among FCMD, MDC1A, and normal

Table 2b
Genes down-regulated in both FCMD and MDC1A skeletal muscle

Genbank Nos.	Product	Common name	Fold change	
			FCMD	MDC1A
Muscle components				
NM_000257	Myosin, heavy polypeptide 7, cardiac muscle, β	*MYH7*	0.01	0.01
NM_003673	Titin-cap (telethonin)	*TCAP*	0.02	0.01
NM_001927	Desmin	*DES*	0.01	0.02
NM_017534	Myosin, heavy polypeptide 2, skeletal muscle, adult	*MYH2*	0.02	0.01
NM_005963	Myosin-binding protein C, fast-type	*MYH1*	0.02	0.01
NM_000232	Sarcoglycan, β	*SGCB*	0.03	0.05
NM_001103	Actinin, α2	*ACTN2*	0.04	0.02
NM_004533	Myosin-binding protein C, fast-type	*MYBPC2*	0.09	0.03
NM_003283	Troponin T1, skeletal, slow	*TNNT1*	0.32	0.5
NM_001100	α1 actin precursor	*ACTA1*	0.06	0.03
X04201	Skeletal muscle tropomyosin	*AA 1-285*	0.14	0.31
Cell differentiation and adhesion				
NM_001958	Eukaryotic translation elongation factor 1 α 2	*EEF1a2*	0.03	0.01
NM_002654	Pyruvate kinase, muscle	*PKM2*	0.05	0.02
NM_053013	Enolase 3	*ENO3*	0.09	0.03
NM_000237	Lipoprotein lipase precursor	*LPL*	0.18	0.45
BC007810	Calpain 3, (p94)	*CALP 3*	0.17	0.12
Energy metabolism				
NM_001824	Creatine kinase, muscle	*CKM*	0.12	0.05
NM_000034	Aldolase A	*ALDOA*	0.21	0.07
NM_004320	ATPase, Ca^{++} transporting, fast twitch 1	*ATP2a1*	0.19	0.05
Others, EST				
NM_016172	Putative glialblastoma cell differentiation-related	*GDBR1*	0.21	0.1
NM_004468	Four and a half LIM domains 3	*FHL3*	0.05	0.03
NM_001449	Four and a half LIM domains 1	*FHL1*	0.07	0.07
NM_005053	RAD23 (*Saccharomyces cerevisiae*) homolog A	*RAD23a*	0.08	0.03
NM_004305	Bridging integrator 1	*BIN1*	0.11	0.05
J03077	Human co-β glucosidase	*Glba*	0.09	0.04
XM_054526	Z-band alternatively spliced PDZ-motif	*ZASP*	0.12	0.09
XM_058642	Similar to adenylosuccinate synthetase	*loc122622*	0.13	0.09
XM_035635	Hypothetical protein DKFZp762M136	*dkfzp762M136*	0.13	0.09
NM_005061	Ribosomal protein L3-like	*RPL31*	0.13	0.17
AA164729	Similar to contains Alu repetitive element	*PTR5*	0.13	0.22
AW755254	Similar to CMYA5 Cardiomyopathy associated gene 5	*CMYA5*	0.2	0.15
XM_034768	Hypothetical protein XP_034768	*PDE4DIP*	0.21	0.18

Table 3a
Selected genes discerning expression in FCMD and MDC1A versus normal muscle

Genbank Nos.	Common	Product
FCMD and MDC1A specific genes		
Up-regulated		
X02508	*ACHR*	Acetylcholine receptor (AChR) α subunit
NM_000090	*COL3a1*	α1 type III collagen preproprotein
NM_000079	*CHRNA1*	Cholinergic receptor, nicotinic, α polypeptide 1 (muscle)
NM_003248	*THBS4*	Thrombospondin 4
NM_003380	*VIM*	Vimentin
XM_049131	*TRA1*	Hypothetical protein XP_049131
NM_005507	*CFL1*	Cofilin 1 (non-muscle)
NM_000041	*APOE*	Apolipoprotein E
NM_003186	*TAGLN*	Transgelin
L01124	*RPS13*	Ribosomal protein S13
NM_004615	*TM4SF2*	Transmembrane 4 superfamily member 2
NM_004997	*MYBPH*	Myosin-binding protein H
Down-regulated		
NM_000232	*SGCB*	Sarcoglycan, β (43kD dystrophin-associated glycoprotein)
NM_003673	*TCAP*	Titin-cap (telethonin)
NM_031287	*MGC3133*	Hypothetical protein MGC3133
NM_000382	*ALDH3a2*	Aldehyde dehydrogenase 3A2
NM_015994	*ATP6m*	Vacuolar proton pump delta polypeptide
NM_014944	*KIAA0911*	KIAA0911 protein
NM_013383	*TCFL4*	MAX-like bHLHZIP protein
NM_004468	*FHL3*	Four and a half LIM domains 3

controls. Any two paired samples showed high correlation co-efficiency (Table 1). The upper right columns indicate the correlation of the actual fold increase or decrease data (Pearson's correlation) and the lower left columns represent the ranking of fold change data (Spearman's correlation). Correlation coefficients for each average fold ratio and the ranking score between F1–F4 and M1 were as high as 0.91 and 0.86, respectively (Table 1, Fig. 2C). These data demonstrate that overall gene expression in these CMDs is similar regardless of age difference, pathological change or type of CMD.

Expression of ECM-related genes is highly elevated, whereas that of mature muscle components is down-regulated in CMDs

Differentially expressed genes were categorized by the function of the encoded protein according to the Gene Ontology classification (e.g., muscle component, ECM component, cell adhesion and growth, inflammation, cellular metabolism, immune response, EST, etc.). For all four CMD individuals, the average ratio of normalized signal intensities relative to normal controls was estimated as a fold change (Tables 2a and 2b).

The vast majority of up-regulated genes in FCMD and MDC1A encode ECM components (Table 2a). This bias is prominent compared to DMD profiles, which show increased expression of genes encoding skeletal muscle components [22]. ECM genes up-regulated in CMDs include *thrombospondin 4*, *collagen3a1*, *collagen15a1*, *osteoblast-specific factor*, *matrix glia protein*, and *lumican* (Table 2a). The high expression of ECM genes presumably is related to fibrotic change, as shown in Fig. 1A. However, expression of fibronectin receptor *integrin 5α*, which is typically up-regulated due to inflammation or fibrosis, showed only a mild increase (1.09 average fold ratio to control in FCMD samples). This observation implies that fibrosis in CMD muscles might result from additional factors to chronic inflammation or muscle fiber degeneration. Genes encoding basement membrane components such as *tenascin*, *laminin receptor-1*, *laminin β*, and *integrin α7* also were up-regulated, as was *DAG1*, which encodes α and β-DG (Table 2a).

Increased expression of the muscle components γ *actin-1*, *myelin basic protein*, *tropomyosin*, and *sarcosin* was observed in the CMDs. Other muscle components, including *myosin heavy chain 2* and *7*, *nebulin*, *titin*, and *desmin*, showed much lower expression levels in CMDs relative to controls (Table 2b). These observations are consistent with previously published expression profiles of DMD muscles [22]. Although some genes encoding components of mature muscle fibers, such as *myosin light chain4* or, *cardiac actinα*, are up-regulated in DMD (Table 4-2, and [22]), these genes were not up-regulated in CMDs. Up-regulation of genes encoding muscle fiber components in DMD generally reflects active regeneration following muscle fiber degeneration. Our observations indicate that muscle degeneration and regeneration are less active in CMDs. Moreover, genes related to cell metabolism, such as *phosphofurkutokinase* and *aldolase*, were substantially down-regulated, suggesting that the total energy metabolism in CMD muscle fibers is likely reduced (Table 2b).

In summary, expression profiling revealed two characteristics. First, most up-regulated genes were ECM

components that may be related to rich interstitial tissues in CMDs. Second, mature muscle components were extremely down-regulated in CMDs. Our data are consistent with the histological finding that the primary feature of CMDs is interstitial fibrosis without muscle degeneration and regeneration.

The Distillation extracted up-regulated ECM genes and suppressed muscle structural genes in CMDs

Bioinformatics using multi-dimensional analysis allowed detection of gene clusters whose expression patterns might help explain CMD pathogenesis [24,25]. We adopted an original statistical analysis method, the Distillation, to extract genes whose expression signals significantly distinguish FCMD, MDC1A, and normal skeletal muscle [23]. Using this method, genes were extracted either as a single gene or as paired genes showing significant expression tendencies between samples tested.

We first analyzed microarray data for genes that distinguish the CMD samples from normal skeletal muscle. From 2345 genes tested, 20 genes were extracted (Table 3a). These include *achr*, *col3a1*, and *thbs4*, which were up-regulated in CMDs. β-Sarcoglycan and *telethonin*, which encode mature muscle components, were down-regulated (Fig. 3A).

Next, we extracted 20 genes that distinguish FCMD from MDC1A and normal controls (Table 3b). Up-regulated genes within this group included *hla-drw1*, *hla-drb3 TNNT-2*, and *lamα2*. In addition, 10 genes paired with *MYH7* were extracted, nine of which have unknown functions (Table 3b). When signals for these pairs are plotted on two-dimensional graphs, distinct expression tendencies become apparent within each disease group (Fig. 3B). These genes might be functionally linked to *MYH7* and contribute to molecular mechanisms underlying FCMD. *CGI-38 brain-specific protein* of unknown function was selected since its expression in MDC1A is distinct from other groups. Nine genes, including *myogenin* and *thyroid hormone binding protein*, were extracted in pair with *CGI-38* (Table 3c).

To find genes specifically involved in these CMDs compared to classical muscular dystrophy, we compared FCMD expression profiles with previously reported DMD profiles [22]. Genes including *chnra, thsb4*, *col3a*, *col15a1*, and *hla-drw12* (Table 4a) were found to be up-regulated in FCMDs and down-regulated in DMD. The genes *actc2*, *actg1 MYH7, MYH2*, and *MYH1* (Table 4b) were down-regulated in FCMD and up-regulated in DMD. These results corroborate the general finding that genes up-regulated in FCMD are mainly ECM components, whereas down-regulated genes tend to be muscle components, differentiating FCMD from DMD.

To confirm the microarray data, we performed real-time quantitative PCR for several selected genes extracted by the Distillation (Figs. 4A and B). This experiment replicated the distinct gene expression patterns seen in CMDs

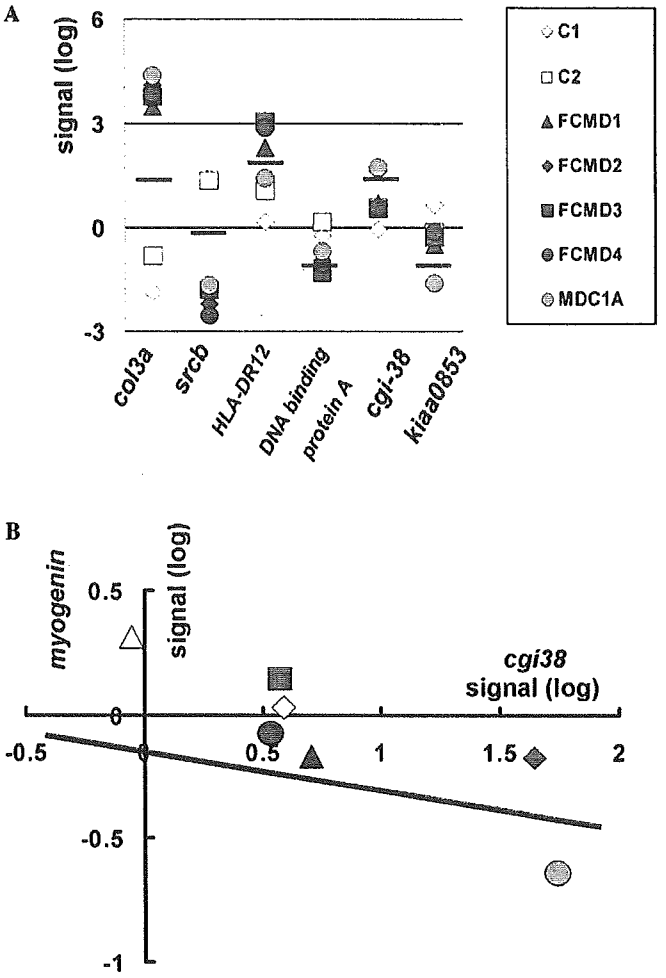

Fig. 3. The Distillation. (A) Several genes sorting FCMD, MDC1A, and normal controls are selected (blue lines). The vertical line shows log scaled signal expression for each gene. *Col3a* and *srcβ* are isolated in the expression profiles of FCMD and MDC1A versus normal control muscle. *HLADR12* and *DNA binding protein A* also discern FCMD from MDC1A and normal muscle; likewise, *CGI-38* and *kiaa 0853* show distinct expression patterns in MDC1A compared to FCMD and normal control. (B) Paired genes sorting FCMD and MDC1A from normal muscle. The horizontal line shows log scaled signal expression of *CGI-38*, and the vertical line shows signal expression of *myogenin*. Note that expression signals of these genes two-dimensionally separate disease groups, suggesting the possibility of linked interactions between these genes.

compared to DMD or normal muscle, demonstrating the reliability of the Distillation as well as the microarray analysis itself. Therefore, these extracted genes likely reflect the unique features of FCMD and MDC1A.

Characteristics of CMDs include elevated expression of muscle cell ECM components

FCMD gene expression profiles were quite similar regardless of age differences or muscle pathology among samples. Since muscle content and fibrotic components vary among patients, we normalized gene expression signals by dividing each signal by the gross area of each muscle component according to the data in Fig. 1B. When

signals in different stages of FCMD were proportionally normalized, gene expression patterns of muscle components such as *myosin light chain 1* and *actin* γ stabilized across samples F1–F4 (Fig. 5). Genes related to muscle fiber components in FCMD seem to be stably expressed irrelevant of muscle fiber content. On the other hand, normalizing expression in FCMD relative to the gross area of interstitial tissue did not stabilize the tendency toward ECM component expression, suggesting that expression of ECM genes does not correlate proportionally with the severity of fibrotic change (Fig. 5). These results imply that expression of fibrotic components in FCMD might not arise from dystrophic change but instead is related to muscle component expression. The high and stable expression of ECM components among all samples indicates that fibrosis is active from very early infancy and may last throughout the disease course.

To clarify which cells express ECM components in FCMD muscles, in situ hybridization was performed for the up-regulated ECM genes *col3a*, *col15a1*, *OSF-2*, and *thbs4*. Surprisingly, these components were expressed primarily by muscle fibers in FCMD, particularly from small-sized, immature muscle cells and satellite cells (Fig. 6), and only slightly by fibroblasts within fibrous tissue. This suggests that the fibrotic change in CMDs is a primary phenotype rather than a secondary effect of chronic inflammation, as is seen in classical muscular dystrophy. Taken together, these results indicate that FCMD and MDC1A can be characterized as active fibrotic disease with suppressed muscle regeneration.

Discussion

Extraction of disease determinant genes using the Distillation

Analysis of gene expression in various tissues or cell samples has evolved from assessment of select target genes to more efficient, high-throughput genomewide screening. Microarray technology can provide valuable insight into important biological and pathological mechanisms and aid in identifying disease-causing genes [25,26]. However, the most emergent challenge in microarray analysis is separating valid data from the 'noise' that inevitably exists in the vast amount of redundant data produced by high-throughput screening. If genes identified through microarray analysis have a true correlation, determining what is statistically 'not true' is another issue. Bioinformatics has made it possible to address such problems by isolating statistically distinct genes [23]. The Distillation (also called TidalSMP, [23]) is a proven method for sorting reliable disease-specific genes using an original, efficient algorithm for mining association rules to determine a correlation.

The dystrophin–glycoprotein complex is a multi-subunit complex, comprised of sarcoplasmic and integral

Table 3b
Selected genes discerning expression in FCMD versus MDC1A and normal muscle

Genbank	Common	Product
FCMD-specific genes		
Up-regulated		
M27635	*HLA-drw12*	Lymphocyte antigen
NM_022555	*HLA-drb3*	Major histocompatibility complex, class II, DR β 3
XM_009540	*KIAA0255*	KIAA0255 gene product
NM_000364	*TNNT2*	Troponin T2, cardiac
NM_000237	*LPL*	Lipoprotein lipase precursor
NM_000426	*Lama2a*	Laminin, α-2 (merosin)
Down-regulated		
NM_000257	*MYH7*	Myosin, heavy polypeptide 7, cardiac muscle, beta
L29073	*EST*	DNA-binding protein a
AL043327	*DKFZP434o1923*	
XM_035662	*LOC137597*	Similar to cathepsin B (H. sapiens)
Down-regulated paired genes		
NM_000257	*MYH7*	Myosin, heavy polypeptide 7, cardiac muscle, beta
and		
NM_017751	*flj20297*	
AF126008	*BRX*	Hypothetical protein FLJ20297
XM_044630	*DKFZP434c131*	Breast cancer nuclear receptor-binding auxiliary protein
BM458054	*EST*	DKFZP434C131 protein
AL157455	*DKFZP761i1912*	IMAGE:553039
XM_042323	*KIAA0833*	EST
NM_014815	*KIAA0130*	KIAA0833 protein
AI401562	*EST*	KIAA0130 gene product
XM_001928	*LOC55924*	IMAGE:2110120
NM_005206	*CRK*	Hypothetical protein

Table 3c
Selected genes discerning expression in MDC1A versus FCMD and normal muscle

Genbank Nos.	Common	Product
MDC1A-specific genes		
Up-regulated		
NM_006471	*MLCB*	Myosin, light polypeptide, non-sarcomeric (20kD)
NM_016140	*LOC51673*	CGI-38 brain-specific protein
Down-regulated		
NM_015070	*KIAA0853*	KIAA0853 protein
XM_012618	*MYH2*	Myosin, heavy polypeptide 2, skeletal muscle, adult
BC004541	*IMAGE:3951723*	Unknown (protein for IMAGE:3951723)
NM_000389	*CDKN1a*	Cyclin-dependent kinase inhibitor 1A
BC008069	*SH3-like*	Similar to src homology three and cysteine rich domain
NM_002479	*MYOG*	MYF4; Myogenic factor-4
NM_006813	*PROL2*	Proline rich 2
NM_000690	*ALDH2*	Aldehyde dehydrogenase 2, mitochondrial
XM_058387	*ANK1*	Ankyrin 1, isoform 8
XM_008333	*ACADVL*	Acyl-Coenzyme A dehydrogenase, very long chain precursor
XM_013017	*KIAA0153*	Hypothetical protein XP_013017
U94777	*PYGM*	Muscle glycogen phosphorylase
NM_004543	*NEB*	Nebulin
NM_003637	*itga10*	Integrin, α 10
Up-regulated	Paired genes	
NM_016140	*LOC51673*	CGI-38 brain-specific protein
Down-regulated, paired with LOC51673		
NM_002479	*MYOG*	Myogenin
NM_001104	*ACTN3*	Skeletal muscle-specific actinin, α 3
NM_015380	*CGI-51*	CGI-51 protein
NM_002826	*QSCN6*	Quiescin Q6
J02783	*P4hb*	Thyroid hormone binding protein precursor
NM_000884	*IMPDH2*	IMP (inosine monophosphate) dehydrogenase 2
NM_013400	*RIP60*	Replication initiation region protein (60kD)
NM_015070	*KIAA0853*	KIAA0853 protein
NM_000257	*MYH7*	Myosin, heavy polypeptide 7, cardiac muscle, beta

Table 4a
Genes up-regulated in FCMD and down-regulated in DMD

Genbank Nos.	Product	Common name	Fold increase	
			FCMD	DMD
XM_005592	Collagen, type XV, α1	*COL15A1*	2.86	0.43
NM_002229	Jun B proto-oncogene (JUNB)	*JUNB*	2.80	0.70
NM_002402	Mesoderm-specific transcript (mouse) homolog (MEST),	*MEST*	2.61	0.53
NM_024416	Osteoglycin (osteoinductive factor, mimecan) (OGN)	*OGN*	2.59	0.43
NM_000090	Collagen, type III, α1	*COL3A1*	2.42	0.29
X64875	Insulin-like growth factor binding protein-3	*IGFBP-3*	2.27	0.85
NM_006475	Osteoblast-specific factor 2 (fasciclin I-like) (OSF-2)	*OSF-2*	2.08	0.14
NM_000079	Cholinergic receptor, nicotinic, α polypeptide 1	*CHRNA1*	2.01	0.64
M27635	MHC HLA-DRw12 allele mRNA, β-1 chain	*HLA-DRW12*	2.01	0.56
NM_001731	B-cell translocation gene 1, anti-proliferative (BTG1)	*BTG1*	1.99	0.56
XM_004063	Early growth response 1 (EGR1)	*EGR1*	1.98	0.65

membrane proteins that link the cytoskeleton to the ECM [27]. This complex is thought to provide mechanical reinforcement for the sarcolemma and to maintain membrane integrity during cycles of muscle contraction and relaxation. It is known that DG spans the sarcolemma, linking extracellular laminin-α2 with dystrophin/cytoskeleton [17]. Defects in this linkage cause muscular dystrophies, as seen in FCMD and MDC1A [4,5,28]. In this sense, the molecular mechanisms underlying FCMD and MDC1A should be similar. Indeed, gene expression profiles in these disorders are virtually the same. However, using the Distillation, we extracted a number of differentially expressed genes, including some with unknown function.

FCMD and MDC1A as primary fibrosis diseases

Upon histological examination, DMD skeletal muscle fibers showed muscle degeneration and active regeneration.

Table 4b
Genes up-regulated in DMD and down-regulated in FCMD

Genbank Nos.	Product	Common name	Fold change	
			FCMD	DMD
NM_001615	Actin, γ2, (ACTG2), mRNA	*ACTG2*	0.45	8.85
NM_001614	Actin, γ1 (ACTG1)	*ACTG1*	0.55	4.42
XM_005368	Protein kinase PKNbeta (pknbeta)	*PKNBETA*	0.91	4.02
NM_005729	Peptidylprolyl isomerase F (cyclophilin F) (PPIF)	*PPIF*	0.77	2.92
NM_000257	Myosin, heavy polypeptide 7, cardiac muscle, β (MYH7)	*MYH7*	0.63	2.82
XM_027916	HP1-BP74 (HP1-BP74)	*HP1-BP74*	0.50	2.74
NM_002476	Myosin, atrial/fetal muscle, light chain; embryonic (MYL4)	*MYL4*	0.48	2.46
NM_001912	Cathepsin L (CTSL)	*CTSL*	0.83	2.13
NM_005963	Myosin heavy chain IIx/d; skeletal muscle, adult (MYH1)	*MYH1*	0.78	1.91
NM_001927	Desmin, (DES)	*DES*	0.72	1.51
NM_001614	MyHC-IIa; MYHas8; MyHC-2A; myosin, heavy polypeptide 2, skeletal muscle, adult (MYH2)	*MYH2*	0.76	1.33

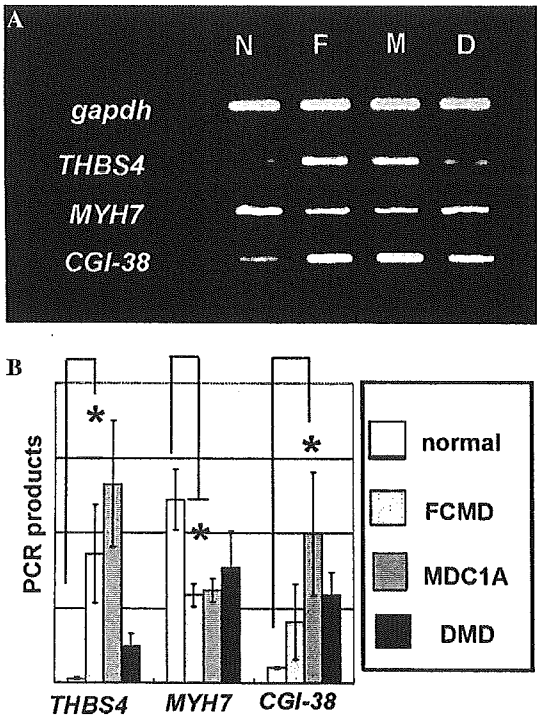

Fig. 4. Gene expression tendencies in CMDs show elevated ECM component expression and low expression of muscle components. (A) Ethidium bromide staining shows up-regulation of *THBS4* and *CGI-38* in FMCD and MDC1A compared to normal muscle and DMD. *MYH7* is down-regulated in FCMD and MDC1A, unlike DMD and normal muscle. (B) Quantitative real-time PCR analysis of mRNA expression. White bar, normal controls; dotted bar, FCMD; gray bar, MDC1A; and black bar, DMD. PCR products are plotted as values normalized to *gapdh*. Each bar represents the mean value of two patients' data. $^*p < 0.005$ (Student's *t* test).

At the molecular level, expression profiling reveals the up-regulation of genes encoding muscle structural proteins, myogenic factors, and immune responses [20,21]. Changes in expression of these genes reflect the clinical phases and histological changes indicating disease progression.

In contrast, our data demonstrate that some of the muscle component genes that are up-regulated in DMD [22] were extremely down-regulated in CMDs. This observation implies less active regeneration of muscle fibers in CMDs. Instead, expression of genes encoding ECM components was substantially high in CMDs. ECM genes are also highly expressed in DMD muscles, generally reflecting a response to necrotic changes in muscle fibers resulting from inflammation. ECM gene expression increases as muscle fibrosis develops due to chronic inflammation at later stages of DMD [22]. In contrast, expression levels of ECM genes in CMD were consistent regardless of histological changes. Further, the elevated ECM genes are not expressed by fibroblasts but by muscle cells themselves. This persistently high expression of ECM genes may be indicative of the primary etiology of CMD.

It has been postulated that dysfunction of *fukutin* in FCMD or laminin-α2 in MDC1A induces severe muscular dystrophy by attenuating stable connections between the skeletal muscle sarcoplasmic membrane and the basement membrane. Indeed, defects in the basement membrane have been reported in FCMD muscle [29]. Basement membrane is thought to not only maintain cell integrity but also to mediate signal transmission in cell differentiation, growth, attachment, survival, polarity, proliferation, and apoptosis [30–32]. We hypothesize that up-regulation of ECM genes observed in these experiments might arise from signal transduction defects due to basement membrane dysfunction.

Regarding the histological characteristics of CMD muscle, one possible explanation for disease etiology is apoptosis of muscle cells. Laminin-α2 is required for myotube survival in vitro [31], and increased apoptotic cells cause embryonic lethality in *fukutin*-null mice due to aberrant basement membrane formation [33]. These findings indicate that the basement membrane is essential to cell survival. Reduction of α-DG in myotubes in vitro also results in reduced levels of laminin expression on cell surfaces and an increase in apoptotic cell death [34]. Hence in normal conditions, connection of laminin and α-DG might be involved in skeletal muscle cell survival. It might be reasonable to imagine that connective tissue simply fills the space created by apoptosis. It is also possible that muscle fibers keeps high transcription levels of ECM to create basement membrane components.

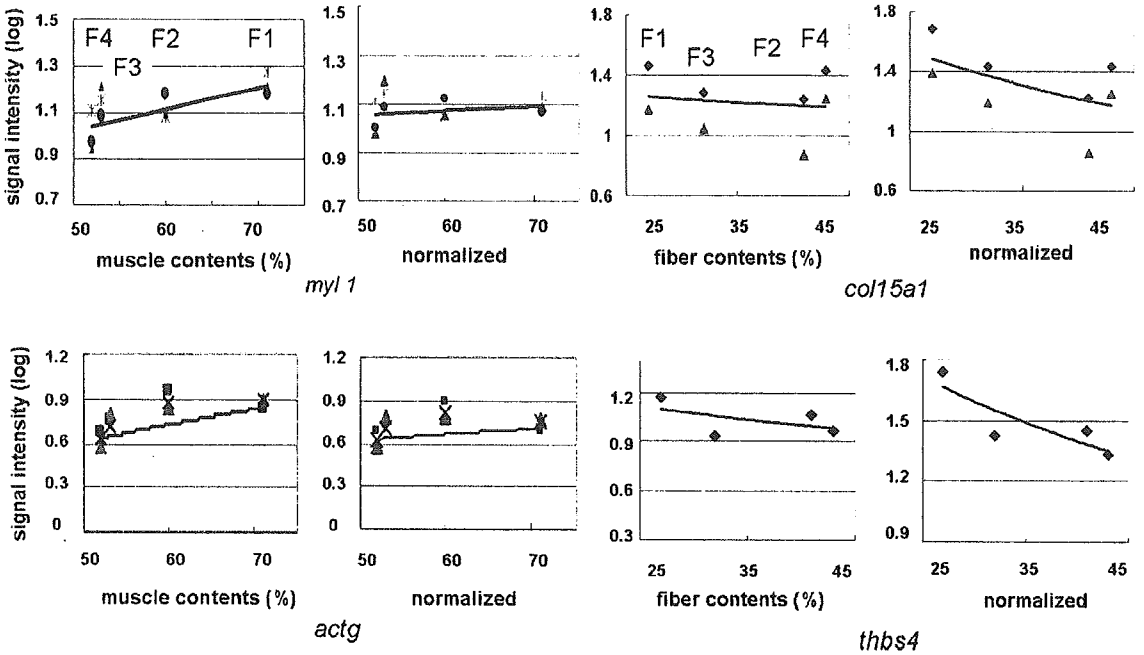

Fig. 5. Gene expression of ECM and muscle component normalized by the area of each component. Each dot shows expression signals of each gene. Each line shows the approximate curves of these signals. *X*-axis, percentage of tissue muscle and interstitial tissue of F1–F4; *Y*-axis, signal intensities of each gene (log scale).

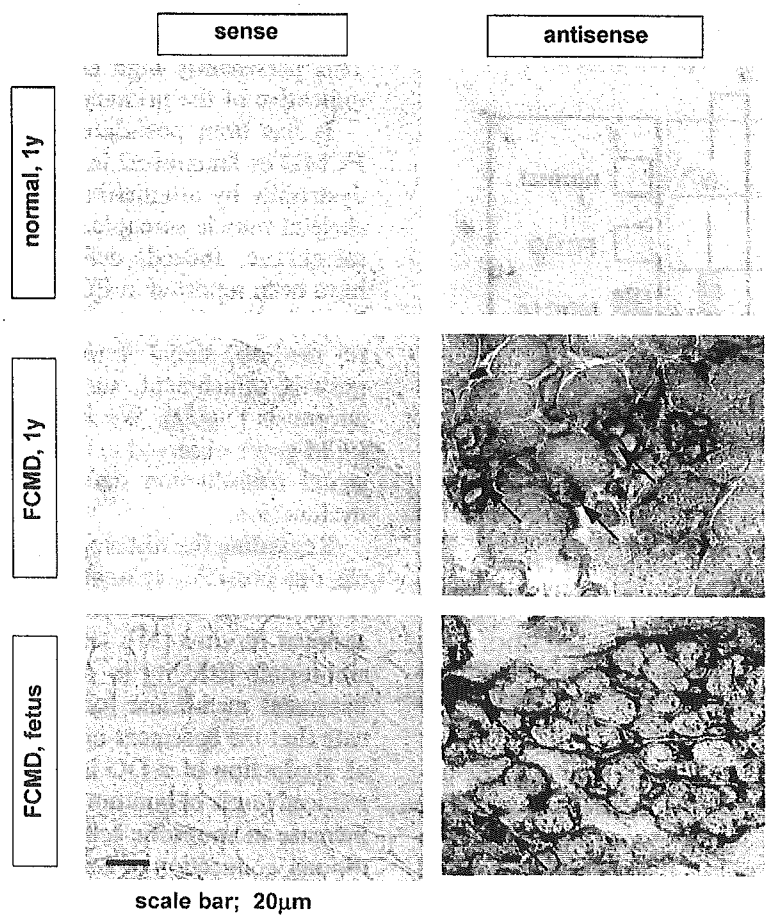

Fig. 6. In situ hybridization of *THBS4* in FCMD skeletal muscle versus normal controls. Upper columns show normal skeletal muscle fibers (1 year of age). No significant *THBS4* signals are seen in muscle fibers (upper right column). Middle columns show FCMD muscle fibers (1 year of age). Bottom columns show fetal (19 weeks) FCMD skeletal muscle. Note that skeletal muscle fibers with small muscle diameters stain positively (arrows) both in FCMD and in fetal tissue (middle and lower right columns). *Col3a*, *col15a*, and *OSF2* show the same results (data not shown). Note that immature muscle fibers, not fibroblasts, express ECM components at high levels.

Alternatively, the differentiation defect in muscle cells might underlie the etiology of these CMDs. Skeletal muscle fibers in FCMD are generally very small, round, and disorganized. Most muscle fibers in CMDs remain small and disorganized with remarkable size diversity. In contrast, regenerating DMD muscle fibers never fail to achieve normal fiber sizes. Skeletal muscle fibers in FCMD somewhat resemble those in fetal skeletal muscle ([35] and unpublished data). Fetal muscle is characterized by premature, small muscle fibers with a high nucleus-to-cytoplasm ratio, rather rich in cell-to-cell intervals with loose muscle bundles. FCMD and MDC1A skeletal muscle fibers might also be in the developmental period of myotubes and muscle fibers, which have substantial space for interstitial ECM components. ECM genes could be up-regulated to promote differentiation of immature muscle cells. It is possible that the delay in differentiation due to the basement membrane defect is significant in the etiology of the CMDs. We presume that maturational arrest is a key factor, followed by up-regulation of ECM components. We have also found neuromuscular junction abnormalities in FCMD (unpublished data) as also have been seen in MDC1A [36]. Since neuromuscular junction formation normally occurs in tandem with basement membrane formation, nerve innervations may also play an important role in muscle differentiation (unpublished data).

Taken together, our observations suggest that the fibrotic change seen in CMDs reflects a primary fibrosis disease rather than the secondary change, as is seen in classical muscular dystrophy. The causes for up-regulation of ECM genes in FCMD and MDC1A muscle merit further scrutiny and may reveal more precise mechanisms for FCMD and MDC1A.

Acknowledgments

We are grateful to Dr. Ikuya Nonaka and Dr. Shin'ichi Takeda for their critical comments and advice, and Dr. Hidetoshi Taniguchi and Dr. Masako Taniike for technical support. We also thank Dr. Jennifer Logan for editing the manuscript. This work was supported by a Health Science Research Grant, Research on Psychiatric and Neurological Diseases and Mental Health and by a Research Grant for Nervous and Mental Disorders (14B-4 and 17A-10), both from the ministry of Health, Labor and Welfare of Japan; and by the 21st Century COE program from the Ministry of Education, Culture, Sports, Science, and Technology of Japan.

References

[1] Y. Fukuyama, M. Osawa, H. Suzuki, Congenital progressive muscular dystrophy of the Fukuyama type-clinical, genetic, and pathological considerations, Brain Dev. 3 (1981) 1–29.

[2] T. Toda, M. Segawa, Y. Nomura, I. Nonaka, K. Masuda, T. Ishihara, M. Suzuki, I. Tomita, Y. Origuchi, K. Ohno, N. Misugi, Y. Sasaki, K. Takada, M. Kawai, K. Otani, T. Murakami, K. Saito, Y. Fukuyama, T. Shimizu, I. Kanazawa, Y. Nakamura, Localization of a gene for Fukuyama type congenital muscular dystrophy to chromosome 9q31–33, Nat. Genet. 3 (1993) 283–286.

[3] K. Kobayashi, Y. Nakahori, M. Miyake, K. Matsumura, E. Kondo-Iida, Y. Nomura, M. Segawa, M. Yoshioka, K. Saito, M. Osawa, K. Hamano, Y. Sakakihara, I. Nonaka, Y. Nakagome, I. Kanazawa, Y. Nakamura, K. Tokunaga, T. Toda, An ancient retrotransposal insertion causes Fukuyama-type congenital muscular dystrophy, Nature 394 (1998) 388–392.

[4] Y.K. Hayashi, M. Ogawa, K. Tagawa, S. Noguchi, T. Ishihara, I. Nonaka, K. Arahata, Selective deficiency of alpha-dystroglycan in Fukuyama-type congenital muscular dystrophy, Neurology 57 (2001) 115–121.

[5] D. Michele, E.R. Barresi, M. Kanagawa, F. Saito, R.D. Cohn, J.S. Satz, J. Dollar, I. Nishino, R.I. Kelley, H. Somer, V. Straub, K.D. Mathews, S.A. Moore, K.P. Campbell, Post-translational disruption of dystroglycan-ligand interactions in congenital muscular dystrophies, Nature 418 (2002) 417–422.

[6] P.K. Grewal, J.E. Hewitt, Glycosylation defects: a new mechanism for muscular dystrophy? Hum. Mol. Genet. 12 (2003) 259–264.

[7] F. Muntoni, M. Brockington, D.J. Blake, S. Torelli, S.C. Brown, Defective glycosylation in muscular dystrophy, Lancet 360 (2002) 1419–1421.

[8] A. Yoshida, K. Kobayashi, H. Manya, K. Taniguchi, H. Kano, M. Mizuno, T. Inazu, H. Mitsuhash, S. Takahashi, M. Takeuchi, R. Herrmann, V. Straub, B. Talim, T. Voit, H. Topaloglu, T. Toda, T. Endo, Muscular dystrophy and neuronal migration disorder caused by mutations in a glycosyltransferase, POMGnT1, Dev. Cell 1 (2001) 717–774.

[9] D. Beltrán-Valero de Bernabé, S. Currier, A. Steinbrecher, J. Celli, E. van Beusekom, B. van der Zwaag, H. Kayserili, L. Merlini, D. Chitayat, W.B. Dobyns, B. Cormand, A. Lehesjoki, J. Cruces, T. Voit, C.A. Walsh, H. van Bokhoven, H.G. Brunner, Mutations in the *O*-mannosyltransferase gene POMT1 give rise to the severe neuronal migration disorder Walker–Warburg syndrome, Am. J. Hum. Genet. 71 (2002) 1033–1034.

[10] J. van Reeuwijk, M. Janssen, C. van den Elzen, D. Beltran-Valero de Bernabé, P. Sabatelli, L. Merlini, M. Boon, H. Scheffer, M. Brockington, F. Muntoni, M.A. Huynen, A. Verrips, C.A. Walsh, P.G. Barth, H.G. Brunner, H. van Bokhoven, POMT2 mutations cause alpha-dystroglycan hypoglycosylation and Walker Warburg syndrome, J. Med. Genet. 12 (2005) 907–912.

[11] M. Brockington, D.J. Blake, P. Prandini, Mutations in the fukutin-related protein gene (FKRP) cause a form of congenital muscular dystrophy with secondary laminin alpha2 deficiency and abnormal glycosylation of alpha-dystroglycan, Am. J. Hum. Genet. 6 (2001) 1198–1209.

[12] C. Longman, M. Brockington, S. Torelli, C. Jimenez-Mallebrera, C. Kennedy, N. Khalil, L. Feng, R.K. Saran, T. Voit, L. Merlini, C.A. Sewry, S.C. Brown, F. Muntoni, Mutations in the human LARGE gene cause MDC1D, a novel form of congenital muscular dystrophy with severe mental retardation and abnormal glycosylation of alpha-dystroglycan, Hum. Mol. Genet. 12 (2003) 2853–2861.

[13] P.K. Grewal, P.J. Holzfeind, R.E. Bittner, J.E. Hewitt, Mutant glycosyltransferase and altered glycosylation of alpha-dystroglycan in the myodystrophy mouse, Nat. Genet. 28 (2001) 151–154.

[14] F.M. Tome, T. Evangelista, A. Leclerc, Y. Sunada, E. Manole, B. Estournet, A. Barois, K.P. Campbell, M. Fardeau, Congenital muscular dystrophy with merosin deficiency, C.R. Acad. Sci. III 317 (1994) 351–357.

[15] A. Helbling-Leclerc, X. Zhang, H. Topaloglu, C. Cruaud, F. Tesson, J. Weissenbach, F.M. Tomé, K. Schwartz, M. Fardeau, K. Tryggvason, P. Guicheney, Mutations in the laminin alpha 2-chain gene (LAMA2) cause merosin-deficient congenital muscular dystrophy, Nat. Genet. 11 (1995) 216–218.

[16] H. Colognato, D.A. Winkelmann, P.S. Yurchenco, Laminin polymerization induces a receptor-cytoskeleton network, J. Cell Biol. 145 (1999) 619–631.

[17] O. Ibraghimov-Beskrovnaya, J.M. Ervasti, C.J. Leveille, C.A. Slaughter, S.W. Sernett, K.P. Campbell, Primary structure of dystrophin-associated glycoproteins linking dystrophin to the extracellular matrix, Nature 355 (1992) 696–702.
[18] J.M. Ervasti, K.P. Campbell, A role for the dystrophin–glycoprotein complex as a transmembrane linker between laminin and actin, J. Cell Biol. 122 (1993) 809–823.
[19] I. Nonaka, H. Sugita, K. Takada, K. Kumagai, Muscle histochemistry in congenital muscular dystrophy with central nervous system involvement, Muscle Nerve 5 (1982) 102–106.
[20] Y.W. Chen, P. Zhao, R. Borup, E.P. Hoffman, Expression profiling in the muscular dystrophies: identification of novel aspects of molecular pathophysiology, J. Cell Biol. 151 (2000) 1321–1336.
[21] J.N. Haslett, D. Sanoudou, A.T. Kho, R.R. Bennett, S.A. Greenberg, I.S. Kohane, A.H. Beggs, L.M. Kunkel, Gene expression comparison of biopsies from Duchenne muscular dystrophy (DMD) and normal skeletal muscle, Proc. Natl. Acad. Sci. USA 99 (2002) 15000–15005.
[22] S. Noguchi, T. Tsukahara, M. Fujita, R. Kurokawa, M. Tachikawa, T. Toda, A. Tsujimoto, K. Arahata, I. Nishino, cDNA microarray analysis of individual Duchenne muscular dystrophy patients, Hum. Mol. Genet. 12 (2003) 595–600.
[23] J. Sese, S. Morishita, Answering the most correlated N association rules efficiently, Proc. of 6th European Conference on Principles and Practice of Knowledge Discovery in Databases, 2002.
[24] M.Q. Zhang, Large-scale gene expression data analysis: a new challenge to computational biologists, Genome Res. 9 (1999) 681–688.
[25] D.D. Bowtell, Options available—from start to finish—for obtaining expression data by microarray, Nat. Genet. 21 (1999) 25–32.
[26] M. Schena, R.A. Heller, T.P. Theriault, K. Konrad, E. Lachenmeier, R.W. Davis, Microarrays: biotechnology's discovery platform for functional genomics, Trends Biotechnol. 16 (1998) 301–306.
[27] J.M. Ervasti, K.P. Campbell, Membrane organization of the dystrophin–glycoprotein complex, Cell 6 (1991) 1121–1131.
[28] M.D. Henry, K.P. Campbell, A role for dystroglycan in basement membrane assembly, Cell 95 (1998) 859–870.
[29] H. Ishii, Y.K. Hayashi, I. Nonaka, K. Arahata, Electron microscopic examination of basal lamina in Fukuyama congenital muscular dystrophy, Neuromuscul. Disord. 3 (1997) 191–197.
[30] M.W. Cohen, C. Jacobson, E.W. Godfrey, K.P. Campbell, S. Carbonetto, Distribution of alpha-dystroglycan during embryonic nerve-muscle synaptogenesis, J. Cell Biol. 129 (1995) 1093–1101.
[31] P.H. Vachon, F. Loechel, H. Xu, U.M. Wewer, E. Engvall, Merosin and laminin in myogenesis; specific requirement for merosin in myotube stability and survival, J. Cell Biol. 134 (1996) 1483–1497.
[32] J.R. Sanes, The basement membrane/basal lamina of skeletal muscle, J. Biol. Chem. 278 (2003) 12601–12604.
[33] H. Kurahashi, M. Taniguchi, C. Meno, Y. Taniguchi, S. Takeda, M. Horie, H. Otani, T. Toda, Basement membrane fragility underlies embryonic lethality in fukutin-null mice, Neurobiol. Dis. 19 (2005) 208–221.
[34] F. Montanaro, M. Lindenbaum, S. Carbonetto, Alpha-dystroglycan is a laminin receptor involved in extracellular matrix assembly on myotubes and muscle cell viability, J. Cell Biol. 145 (1999) 1325–1340.
[35] H.B. Sarnat, Cerebral dysgenesis and their influence on fetal muscle development, Brain Dev. 8 (1986) 495–499.
[36] P.G. Noakes, M. Gautam, J. Mudd, J.R. Sanes, J.P. Merlie, Aberrant differentiation of neuromuscular junctions in mice lacking s-laminin/laminin beta 2, Nature 16 (1995) 258–262.